Scaling results for charged sectors of near conformal QCD

Jahmall Bersini,[1,*] Alessandra D'Alise,[2,3,5,†] Clelia Gambardella,[3,4,5,‡] and Francesco Sannino[2,3,4,5,§]

[1] *Kavli IPMU (WPI), UTIAS, The University of Tokyo, Kashiwa, Chiba 277-8583, Japan*
[2] *Department of Physics E. Pancini, Università di Napoli Federico II, via Cintia, 80126 Napoli, Italy*
[3] *INFN sezione di Napoli, via Cintia, 80126 Napoli, Italy*
[4] *Scuola Superiore Meridionale, Largo S. Marcellino, 10, 80138 Napoli NA, Italy*
[5] *Quantum Theory Center (ħQTC) at IMADA and D-IAS, Southern Denmark University, Campusvej 55, 5230 Odense M, Denmark*

(Received 30 January 2024; accepted 28 May 2024; published 24 June 2024)

We provide the leading near conformal corrections on a cylinder to the scaling dimension of the lowest-lying fixed isospin charge Q operators defined at the lower boundary of the quantum chromodynamics conformal window, $\tilde{\Delta}_Q = \tilde{\Delta}_Q^* + (\frac{m_\sigma}{4\pi\nu})^2 Q^{\frac{\Delta}{3}} B_1 + (\frac{m_\pi(\theta)}{4\pi\nu})^4 Q^{\frac{2}{3}(1-\gamma)} B_2 + \mathcal{O}(m_\sigma^4, m_\pi^8, m_\sigma^2 m_\pi^4)$. Here, $\tilde{\Delta}_Q/r$ is the classical ground state energy of the theory on $\mathbb{R} \times S_r^3$ at fixed isospin charge while $\tilde{\Delta}_Q^*$ is the scaling dimension at the leading order in the large charge expansion. In the conformal limit $m_\sigma = m_\pi = 0$, the state-operator correspondence implies $\tilde{\Delta}_Q = \tilde{\Delta}_Q^*$. The near-conformal corrections are expressed in powers of the dilaton and pion masses in units of the chiral symmetry breaking scale $4\pi\nu$ with the θ-angle dependence encoded directly in the pion mass. The characteristic Q-scaling is dictated by the quark mass operator anomalous dimension γ and the one characterizing the dilaton potential Δ. The coefficients B_i with $i = 1, 2$ depend on the geometry of the cylinder and properties of the nearby conformal field theory.

DOI: 10.1103/PhysRevD.109.125015

I. INTRODUCTION

Unveiling near conformal properties of quantum chromodynamics (QCD) has attracted much interest over the past several decades. This exploration was spurred by the seminal work of Banks and Zaks [1] who discovered the existence of a perturbative infrared (IR) fixed point in massless QCD for a number of flavors N_f just below the loss of asymptotic freedom. As one decreases N_f relative to the fixed number of colors N_c, one expects below a critical number of flavors N_f^c the theory to undergo a quantum phase transition. That this transition is bound to occur is clear from the fact that, for the observed number of light flavors, the theory breaks chiral symmetry dynamically generating a nonperturbative scale even in the absence of explicit light quark masses. The window in the flavor-color space where the theory displays IR conformality is termed *conformal window,* and the determination of its boundaries constitutes an active area of research [2–16].

Several key questions are related to the dynamics near the lower boundary of the conformal window. These range from a precise determination of its lower edge to the characterization of the quantum phase transition. One exciting possibility concerning the transition is to lose conformality à la Berezinskii-Kosterlitz-Thouless (BKT) [17–19]. The latter occurs in two dimensions and was envisioned for four dimensions in [20–23]. An alternative scenario considers the quantum transition to be a jumping one [24]. The first possibility leads to infrared nonconformal physics displaying premonitory signs of near conformality that can be observed in the power-law scaling of certain phenomenologically relevant operators [25–27]. This dynamics is also known as walking dynamics since the underlying gauge coupling has a region in the renormalization group flow, where the coupling is almost constant and therefore it walks rather than displaying a running behavior. Such a walking behavior has recently been shown to mathematically describe the endemic state of pandemics [28] via the epidemic renormalization group approach [29]. This methodology was also used to successfully predict the second wave COVID-19 pandemic in Europe [30] providing policymakers crucial epidemiological information. In terms of the spectrum of the theory, in the confining and chiral symmetry broken phase occurring below but near the lower end of the conformal window, besides the ordinary

*jahmall.bersini@ipmu.jp
†alessandra.dalise@unina.it
‡c.gambardella@ssmeridionale.it
§sannino@qtc.sdu.dk

Published by the American Physical Society under the terms of the Creative Commons Attribution 4.0 International license. Further distribution of this work must maintain attribution to the author(s) and the published article's title, journal citation, and DOI. Funded by SCOAP³.

Goldstones, it has long been argued [31–34] that another precursor of a smooth quantum phase transition is the occurrence of a dilaton in the theory. Its description at the effective Lagrangian level goes back to the work of Coleman [35] and for walking dynamics has been considered in [4,34,36–38]. Recent investigations via effective approaches in different dynamical regimes have appeared in [39–51]. An explicit calculable example has been discussed in [52], where it was possible to demonstrate the emergence of a dilaton in a near conformal field theory (CFT) alongside a precise study of all the relevant scales emerging once conformality is lost. A complementary analysis of the mass-induced confinement for gauge-fermion theories near the lower edge of the conformal window was performed in [53]. One can also use first principle lattice simulations to disentangle the dilaton properties. However, this is a difficult task since its quantum numbers are the ones of the vacuum, and therefore, it is subject to large numerical noise. Nevertheless, there have been attempts to fit effective approaches to lattice data (see, e.g., [44,54–62]).

Complementary ways to isolate the dilaton properties and more generally, to learn about the near conformal dynamics of QCD are therefore vital to corner the properties of the flavor-driven quantum phase transition. As we shall see, fixed charge sectors offer novel opportunities to investigate near conformal dynamics, providing precious information on the sectors responsible for breaking conformality. We start by recalling that central quantities in any CFT are scaling dimensions of local operators. By the state-operator correspondence [63], these are the energies of the corresponding states on a nontrivial gravitational background. For example, the scaling dimension of the lowest-lying operator of charge Q, denoted with Δ_Q^*, is mapped into the ground state energy E_Q on the cylinder via the relation,

$$\Delta_Q^* = rE_Q, \tag{1}$$

with r the radius of the cylinder. In the large charge limit, we can compute scaling dimensions of fixed charge operators by means of semiclassical computations [64–76]. Intriguingly, the large charge framework allows us to perform analytical calculations in strongly coupled quantum field theories, and its predictions have been tested via numerical Monte Carlo simulations in [65,77–80]. In this work, we follow [49,50,66] and extend this relation to near conformal field theories by introducing the quantity,

$$\Delta_Q \equiv r\,E_Q = \Delta_Q^* + \text{near CFT terms}. \tag{2}$$

The near CFT terms depend on the way the CFT is deformed. In the case at hand, we have two sources of conformal breaking: one stemming from an explicit quark mass term and the other from the occurrence of an operator of dimension Δ inducing a dilaton potential. Therefore, in this work, we extend the chiral Lagrangian to include a dilaton sector and use the large charge expansion framework to compute Δ_Q, arriving at our central result,

$$\tilde{\Delta}_Q = \tilde{\Delta}_Q^* + \left(\frac{m_\sigma}{4\pi\nu}\right)^2 Q^{\frac{\Delta}{3}} B_1 + \left(\frac{m_\pi(\theta)}{4\pi\nu}\right)^4 Q^{\frac{2}{3}(1-\gamma)} B_2 + \mathcal{O}(m_\sigma^4, m_\pi^8, m_\sigma^2 m_\pi^4), \tag{3}$$

where $\tilde{\Delta}_Q/r$ is the classical ground state energy while $\tilde{\Delta}_Q^*$ is the leading order contribution to Δ_Q^* in the large charge expansion. The near-conformal corrections are expressed in powers of the dilaton and pion masses given in units of the chiral symmetry breaking scale $4\pi\nu$. The θ-angle dependence is explicitly encoded in the pion mass. The novel scalings in the charge of the near conformal corrections are expressed in terms of the quark mass operator anomalous dimension γ and the one characterizing the dilaton potential Δ. The coefficients B_i with $i = 1, 2$ depend on the geometry of the cylinder and the properties of the nearby CFT. The above result for $\tilde{\Delta}_Q$ in (3) is obtained as the large charge limit of the general expression given in (41) at the leading order in the semiclassical expansion. The next-to-leading order, to be computed in the future, requires the knowledge of the spectrum of fluctuations that we have also determined here. Additionally, we have also provided the phase diagram of QCD at nonzero isospin chemical potential in the presence of the CP-violating topological term.

The paper is organized as follows. In Sec. II, we introduce the QCD chiral Lagrangian for generic N_f, including the θ-angle and isospin chemical potential μ. The $\mu - \theta$ phase diagram is presented in Sec. III. The dilaton potential and setup for the large charge expansion are discussed in Sec. IV. Section V is devoted to the determination of $\tilde{\Delta}_Q$, while in Sec. VI, we first discuss the patterns of symmetry breaking and then compute the spectrum of fluctuations. Section VII is dedicated to the universal contributions in the conformal limit. We offer our conclusions in Sec. VIII.

II. CHIRAL LAGRANGIAN AT FINITE ISOSPIN AND θ-ANGLE: NOTATION AND CONVENTIONS

The low-energy dynamics of QCD at finite generalized isospin density is described by the chiral Lagrangian below,

$$\mathcal{L} = \nu^2 \mathrm{Tr}\{\partial_\mu \Sigma \partial^\mu \Sigma^\dagger\} + m_\pi^2 \nu^2 \mathrm{Tr}\{M\Sigma + M^\dagger \Sigma^\dagger\} + 2i\mu\nu^2 \mathrm{Tr}\{I\partial_0 \Sigma\Sigma^\dagger - I\Sigma^\dagger \partial_0 \Sigma\} + 2\mu^2\nu^2 \mathrm{Tr}\{II - \Sigma^\dagger I \Sigma I\}, \tag{4}$$

where we use the Lorentzian signature. Here, ν is half the pion decay constant, μ is the (generalized) isospin chemical potential, and

$$\Sigma = e^{i\varphi/\nu}, \qquad \varphi = \Pi^a T^a + \frac{S}{\sqrt{N_f}}, \tag{5}$$

with T^a the $SU(N_f)$ generators normalized as $\mathrm{Tr}\{T^a T^b\} = \delta^{ab}$. The mass matrix and the charge generator read

$$M = \mathbb{1}_{N_f}, \qquad I = \frac{1}{2}\begin{pmatrix} \mathbb{1}_{N_f/2} & 0 \\ 0 & -\mathbb{1}_{N_f/2} \end{pmatrix}, \tag{6}$$

where we assumed degenerate Goldstone bosons of mass m_π. The matrix I generalizes the concept of isospin in the multiflavor theory, with the two flavor case being the conventional QCD isospin. In this work, we will focus on the dynamics of the theory at finite charge density, with the charge defined via the generator I with μ being the associated chemical potential. The relevant power counting is $p^2 \sim m_q \sim \mu^2$ with m_q the quark mass. Since $m_\pi^2 \sim m_q$, this implies that parametrically, we have $m_\pi \sim \mu$.

Finally, as fully detailed in [81,82], the CP-violating topological sector is included through the θ-angle term,

$$\Delta\mathcal{L}_\theta = -a\nu^2\left(\theta - \frac{i}{2}\mathrm{Tr}\{\log\Sigma - \log\Sigma^\dagger\}\right)^2, \tag{7}$$

where a is the topological susceptibility of the underlying Yang-Mills theory. Note that the introduction of the above term is well-justified only in the large number of colors limit. However, in discussing the phase diagram of the theory in the next section, we will work at the leading order in an expansion in m_π^2/a. Since this is equivalent to incorporating the θ-angle directly in the mass term (as done in, e.g., [83–85]) the corresponding analysis does not rely on the large N_c limit. On the other hand, when studying the dispersion relation of the eta prime mode in Sec. VI, the use of the large N_c limit is implied.

III. PHASE DIAGRAM IN THE $\mu-\theta$ PLANE

In the absence of the θ-angle, the ground state of our theory generalizes the $N_f = 2$ case examined in detail in [86] and takes the following form:

$$\Sigma_c = \mathbb{1}_{N_f}\cos\varphi + i\Sigma_I \sin\varphi, \tag{8}$$

with

$$\Sigma_I = \begin{pmatrix} 0 & \mathbb{1}_{N_f/2} \\ \mathbb{1}_{N_f/2} & 0 \end{pmatrix}\cos\eta + i\begin{pmatrix} 0 & -\mathbb{1}_{N_f/2} \\ \mathbb{1}_{N_f/2} & 0 \end{pmatrix}\sin\eta. \tag{9}$$

As shown in [87], the minimization of the potential results from the competition of two terms in the right-hand side of Eq. (8), which individually minimize, respectively, the mass and isospin terms in the potential. Their contribution is weighted by the angle φ, which is determined by the equations of motion (EOMs). Moreover, it can be shown that the isospin term in the potential is minimized when Σ_I satisfies $I\Sigma_I = -\Sigma_I I$. To take into account the effect of the θ-angle on the vacuum state, we introduce the Witten variables α_i [81] and arrive at our ansatz for the ground state,

$$\Sigma_0 = U(\alpha_i)\Sigma_c, \quad \text{with} \quad U(\alpha_i) = \mathrm{diag}\{e^{-i\alpha_1}, \ldots, e^{-i\alpha_{N_f}}\}. \tag{10}$$

It is useful to define the following quantities:

$$\bar{\theta} = \theta - \sum_i^{N_f}\alpha_i, \qquad X = \sum_{i=1}^{N_f}\cos\alpha_i, \tag{11}$$

in terms of which the Lagrangian of the theory evaluated on the ground state ansatz reads

$$\mathcal{L}[\Sigma_0] = 2m_\pi^2\nu^2 X\cos\varphi + N_f\mu^2\nu^2\sin^2\varphi - a\nu^2\bar{\theta}^2. \tag{12}$$

The angle φ and the Witten variables α_i are determined by the EOM as

$$\sin\varphi\left(N_f\cos\varphi - \frac{m_\pi^2 X}{\mu^2}\right) = 0, \tag{13}$$

$$m_\pi^2 \sin\alpha_i\cos\varphi = a\bar{\theta}, \quad i = 1, \ldots, N_f, \tag{14}$$

while the angle η does not appear in the equation of motion, meaning that there is a residual unbroken $U(1)$ isospin vector symmetry. However, choosing a specific value of η amounts to the further spontaneous breaking of this leftover $U(1)$. The first EOM has two solutions, namely, $\varphi = 0$ and $\cos\varphi = \frac{m_\pi^2 X}{N_f\mu^2}$. When the latter is realized, the theory is in a superfluid phase characterized by pion condensation. The energy density of the system in the two phases reads

$$E(\theta) = -2m_\pi^2\nu^2 X + a\nu^2\bar{\theta}^2 \quad \text{normal phase} \quad (\varphi = 0)$$

$$E(\theta) = -\frac{m_\pi^4\nu^2}{N_f\mu^2}X^2 - N_f\nu^2\mu^2 + a\nu^2\bar{\theta}^2$$

$$\text{superfluid phase} \quad \left(\cos\varphi = \frac{m_\pi^2 X}{N_f\mu^2}\right). \tag{15}$$

We first observe that when $a \gg m_\pi^2$ the θ-dependence results in an effective pion mass $m_\pi^2(\theta) = m_\pi^2 X/N_f$. The EOMs and the expression for the vacuum energy of the system are very similar to the ones found in [88] for two-color QCD with finite baryon density. At $\theta = 0$, the normal to superfluid phase transition occurs at a critical value of the chemical potential $\mu_c = m_\pi$. Since the θ-vacuum may differ in the two phases, to study the superfluid transition at nonvanishing values of θ, we first need to determine the θ-dependence. We then solve Eq. (14) by expanding in powers of m_π^2/a that we take to be small. Specifically, at the leading order in m_π^2/a, we have

$$\alpha_i = \begin{cases} \pi - \alpha(\theta), & i = 1, \dots, n \\ \alpha(\theta), & i = n+1, \dots, N_f, \end{cases} \tag{16}$$

where

$$\alpha(\theta) = \frac{\theta + (2k - n)\pi}{(N_f - 2n)}, \quad k = 0, \dots, N_f - 2n - 1, \quad n = 0, \dots, \left[\frac{N_f - 1}{2}\right]. \tag{17}$$

The parameters n and k label the various solutions to the EOMs. The interval of values for k is constrained because at fixed n the solutions are periodic in k of period $N_f - 2n$. In the normal phase, the energy is minimized when X is maximized. As has been shown in [88], the solution minimizing the energy has $n = 0$ and the following values of $\alpha(\theta)$:

$$\alpha(\theta) = \begin{cases} \frac{\theta}{N_f}, & \theta \in [0, \pi] \\ \frac{\theta - 2\pi}{N_f}, & \theta \in [\pi, 2\pi], \end{cases} \tag{18}$$

which correspond, respectively, to $k = 0$ and $k = N_f - 1$.

The physics at $\theta = \pi$ deserves further discussion. In fact, the Lagrangian possesses CP symmetry when $\theta = \pi$ but the latter is spontaneously broken by the vacuum leading to the well-known Dashen's phenomenon [89]. In fact, at $\theta = \pi$, the two solutions for $\alpha(\theta)$ in Eq. (18) have the same energy leading to degenerate vacua connected by a CP transformation. In Fig. 1, we visualize the ground state energy as a function of θ for the template case $N_f = 2$ as well as a plot of the CP order parameter $\langle F\tilde{F}\rangle$ associated with the pseudoscalar glueball condensate.

We now move to the θ-dependence in the superfluid phase. The EOM becomes

$$\frac{m_\pi^4}{N_f \mu^2} X \sin\alpha_i = a\bar{\theta}, \quad i = 1, \dots, N_f, \tag{19}$$

and admits the same solution (17) at the leading order in the natural expansion parameter $\frac{m_\pi^4}{a\mu^2}$. The crucial difference with respect to the normal phase is that the energy now depends quadratically instead of linearly on X. The situation is analogous to the case of two-color QCD at finite baryon charge investigated in detail in [88] for even N_f. As has been found there, the ground state solution is the same as the normal phase being given by Eq. (18). Accordingly, for $N_f > 2$, at the crossing point $\theta = \pi$ spontaneous breaking of CP occurs. On the other hand, for $N_f = 2$, the two solutions $\alpha(\theta) = \frac{\theta}{N_f}$ and $\alpha(\theta) = \frac{\theta - 2\pi}{N_f}$ have degenerate energy for all values of θ. As a consequence, the physics is analytic at $\theta = \pi$ and Dashen's phenomenon does not occur [88,90]. The θ-vacuum in the superfluid phase in the two flavor case is illustrated in Fig. 2.

Note that the pair of completely degenerate solutions remains such to all orders in $\frac{m_\pi^4}{a\mu^2}$. In fact, given the EOM (19) for a certain $\alpha(\theta)$,

$$\frac{m_\pi^4}{2a\mu^2} \sin(2\alpha(\theta)) = \theta - 2\alpha(\theta), \tag{20}$$

we have the same EOM for $\alpha(\theta) + \pi$, upon shifting the θ-angle as $\theta \to \theta + 2\pi$. However, this shift leaves the physics unaltered. Finally, we investigate the critical value of the isospin chemical potential where the superfluid phase

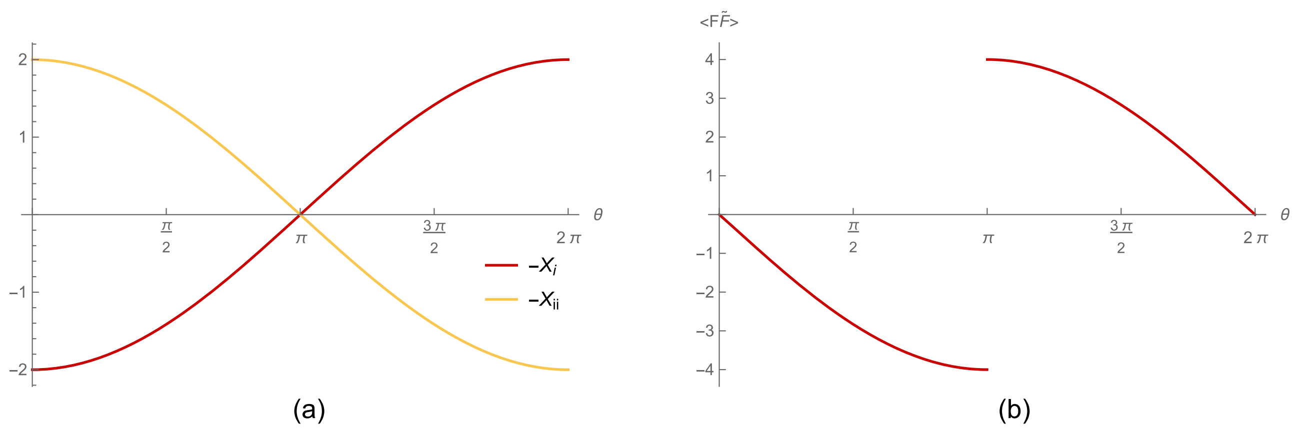

FIG. 1. θ-dependence of the normalized ground state energy and CP order parameter $\langle F\tilde{F}\rangle$ as a function of θ for $N_f = 2$ in the normal phase. Here, $X_i = 2\cos(\theta/2)$ and $X_{ii} = 2\cos(\theta/2 - \pi)$ refers to the two solutions for $\alpha(\theta)$ in Eq. (18). (a) θ-dependence of the energy in the normal phase for $N_f = 2$. (b) CP order parameter for $N_f = 2$.

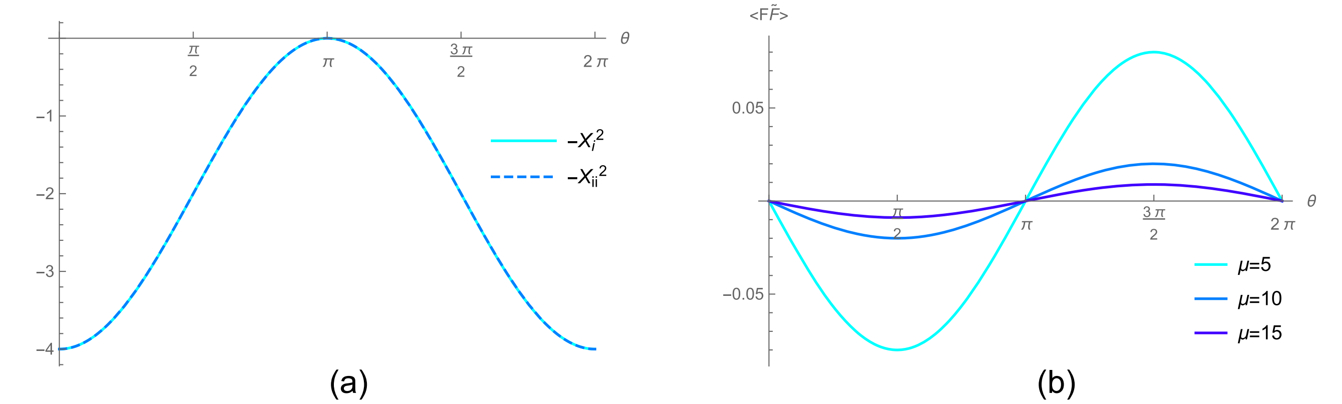

FIG. 2. θ-dependence of the normalized ground state energy and CP order parameter $\langle F\tilde{F}\rangle$ as a function of θ for $N_f = 2$ in the superfluid phase. Here, $X_i^2 = 4\cos^2(\theta/2)$ and $X_{ii}^2 = 4\cos^2(\theta/2 - \pi)$ refers to the two solutions for $\alpha(\theta)$ in Eq. (18) while μ is measured in units of m_π. (a) θ-dependence of the energy in the superfluid phase for $N_f = 2$. (b) CP order parameter for $N_f = 2$.

transition occurs. For $m_\pi^2 \ll a$, the latter occurs at a critical value of the chemical potential given by

$$\mu_c = m_\pi(\theta) = m_\pi\left[\sqrt{\left|\cos\frac{\theta}{N_f}\right|} + \mathcal{O}\left(\frac{m_\pi^2}{a}\right)\right], \quad (21)$$

which is of particular interest when $N_f = 2$ at $\theta = \pi$. In fact, μ_c is almost zero since the effective pion mass $m_\pi^2(\theta) \sim m_\pi^2|\cos(\theta/2)|$ identically vanishes. Concretely, at $\theta \sim \pi$, we have

$$\mu_c \sim m_\pi\sqrt{\frac{m_\pi^2}{a} + \frac{|\phi|}{2}}, \qquad \phi \equiv \theta - \pi. \quad (22)$$

On the other hand, a vanishing pion mass at the effective Lagrangian level raises an apparent paradox since it would imply no explicit breaking of chiral symmetry. However, there is no chiral symmetry restoration in the fundamental QCD Lagrangian at $\theta = \pi$. The apparent paradox is solved by pointing out that the global flavor symmetry is still broken when including higher-order mass terms in the effective Lagrangian as explained in detail in [84,85].

IV. DILATON AUGMENTED CHIRAL LAGRANGIAN AND THE LARGE CHARGE EXPANSION

In this section, following [66], we consider the dynamics near the lower edge of the conformal window to determine the ground state energy of charged states on a nontrivial background that can be associated with scaling dimensions of QCD operators carrying (generalized) isospin charge. The first step is to upgrade the chiral Lagrangian to a conformally invariant theory via the introduction of a scalar degree of freedom σ, the *dilaton*, which under dilations $x \mapsto e^\lambda x$ transforms as

$$\sigma \mapsto \sigma - \frac{\lambda}{f}. \quad (23)$$

Scale invariance can then be enforced at the effective action level by coupling σ to each operator $\mathcal{O}_k$ of dimension k appearing in the Lagrangian as [35,91]

$$\mathcal{O}_k \mapsto e^{(k-4)\sigma f}\mathcal{O}_k. \quad (24)$$

The resulting theory features nonlinearly realized scale invariance with f and σ being the length scale and the Goldstone boson associated with the spontaneous breaking of conformal symmetry, respectively.

Explicit breaking of the latter can be taken into account introducing a potential term for σ. The construction of the dilaton potential and the related power counting has been discussed multiple times in the literature [39,42,44,47,48,58,91]. Several works [39,47,48,91] considered the breaking of conformality as the result of perturbing a CFT with a relevant operator $\mathcal{O}$ with conformal dimension Δ, i.e.,

$$\mathcal{L}_{\mathrm{CFT}} \to \mathcal{L}_{\mathrm{CFT}} + \lambda_{\mathcal{O}}\mathcal{O}, \quad (25)$$

with $\lambda_{\mathcal{O}}$ the corresponding coupling. The generated potential can be written as a power series depending on an infinite number of coefficients as follows:

$$V(\sigma) = f^{-4}e^{-4\sigma f}\sum_{n=0}^{\infty} c_n e^{-n(\Delta-4)f\sigma}, \quad (26)$$

where $c_n \sim \lambda_{\mathcal{O}}^n$ [39,91,92]. When $\lambda_{\mathcal{O}} \ll 1$, the explicit conformal breaking is small, and one can approximate the potential as

$$V(\sigma) = \frac{m_\sigma^2 e^{-4f\sigma}}{4(4-\Delta)f^2} - \frac{m_\sigma^2 e^{-\Delta f\sigma}}{\Delta(4-\Delta)f^2} + \mathcal{O}(\lambda_{\mathcal{O}}^2), \quad (27)$$

which is obtained by retaining only the first two terms in Eq. (26). Then the coefficients c_0 and c_1 are fixed requiring $\sigma_0 \equiv \langle\sigma\rangle = 0$ and defining the dilaton mass as $m_\sigma^2 \equiv \frac{\partial^2 V(\sigma)}{\partial\sigma^2}|_{\sigma=\langle\sigma\rangle}$. Concretely, we have

$$\frac{c_1}{c_0} = -\frac{4}{\Delta}, \quad \text{with} \quad c_0 = \frac{f^2 m_\sigma^2}{4(4-\Delta)}. \tag{28}$$

The potential (27) has been considered in various recent studies of QCD-like theories in the near conformal regime [39,46–48,50,57,93] as well as in the description of dense skyrmion matter [51,94,95]. In the EFT spirit, the nature of the perturbing operator and its scaling dimension Δ is left unspecified.[1] However, the relation (28) breaks the assumed scaling $c_n \sim \lambda_{\mathcal{O}}^n$ of the coefficients of Eq. (26). Moreover, in a renormalizable theory like QCD, the breaking of conformality is expected to stem from the running of the coupling which in turn strongly constrains the form of the potential. In light of these observations, the potential (27) should be seen as a model for the conformal breaking. Another case where the explicit breaking of scale symmetry is small occurs when the perturbing operator $\mathcal{O}$ is nearly marginal. In this case, it is possible to expand Eq. (26) in powers of $(\Delta - 4)$ obtaining

$$V_{\Delta_{\mathcal{O}}\to 4}(\sigma) = -\frac{m_\sigma^2 e^{-4f\sigma}}{16f^2}(1+4f\sigma) + \mathcal{O}((\Delta-4)^2). \tag{29}$$

The above potential has also been constructed in a series of recent papers [42,44,58–61], which make use of the Veneziano limit and assume the following power counting:

$$p^2 \sim m_q \sim (N_f - N_f^c)/N_c \sim 1/N_c. \tag{30}$$

Furthermore, the authors of [42,44,58–61] argued that Eq. (29) is the only consistent potential for QCD-like theories. However, since Eq. (29) can be formally seen as a subcase (the $\Delta \to 4$ limit) of Eq. (27), in what follows, we will assume the generic form of the dilaton potential Eq. (27) in order to keep our analysis as general as possible.

Finally, the mass term operator has dimension $y = 3 - \gamma$, with γ being the anomalous dimension of the chiral condensate.

Our second step is to employ the large charge expansion framework [64,67,74] to determine the scaling dimension Δ_Q^* of the lowest-lying operator with charge Q. To this end, we exploit the approximate Weyl invariance of the near conformal theory to map the latter onto the cylinder $\mathbb{R}\times S_r^3$. We denote the volume, the radius, and the Ricci scalar of S_r^3 as V, r, and $R = \frac{6}{r^2}$, respectively. The advantage is that we can now consider the state-operator correspondence, which links Δ_Q^* to the ground state energy E_Q at fixed Q of the theory on the cylinder as

$$\Delta_Q^* = rE_Q, \qquad E_Q = \mu Q - \mathcal{L}. \tag{31}$$

The dilaton-pion effective Lagrangian on $\mathbb{R}\times S_r^3$ reads

$$\begin{aligned}\mathcal{L}_\sigma = {}& \nu^2 \mathrm{Tr}\{\partial_\mu\Sigma\partial^\mu\Sigma^\dagger\}e^{-2\sigma f} + m_\pi^2\nu^2\mathrm{Tr}\{M\Sigma + M^\dagger\Sigma^\dagger\}e^{-y\sigma f} + 2\mu^2\nu^2\mathrm{Tr}\{II - \Sigma^\dagger I\Sigma I\}e^{-2\sigma f}\\ &+ 2i\mu\nu^2\mathrm{Tr}\{I\partial_0\Sigma\Sigma^\dagger - I\Sigma^\dagger\partial_0\Sigma\}e^{-2\sigma f} - a\nu^2\left(\theta - \frac{i}{2}\mathrm{Tr}\{\log\Sigma - \log\Sigma^\dagger\}\right)^2 e^{-4\sigma f} - \Lambda_0^4 e^{-4\sigma f}\\ &+ \frac{1}{2}\left(\partial_\mu\sigma\partial^\mu\sigma - \frac{R}{6f^2}\right)e^{-2\sigma f} - V(\sigma),\end{aligned} \tag{32}$$

where for later convenience, we included the bare cosmological constant Λ_0. In the conformal limit, $m_\pi = m_\sigma = 0$, Δ_Q^* can then be computed via a semiclassical expansion in the double scaling limit,

$$\Lambda_0 f \to 0, \qquad Q \to \infty, \qquad Q(\Lambda_0 f)^4 = \text{fixed}. \tag{33}$$

This can be seen by considering the expectation value of the evolution operator $U = e^{-HT}$ in an arbitrary state $|Q\rangle$ with charge Q,

$$\langle U\rangle_Q \equiv \langle Q|e^{-HT}|Q\rangle \underset{T\to\infty}{\longrightarrow} \mathcal{N}e^{-E_Q T} = \mathcal{N}e^{-\frac{\Delta_Q^*}{r}T}, \tag{34}$$

with H the Hamiltonian, T the time interval, and $\mathcal{N}$ an unimportant normalization factor. Then one can rescale the fields as $\Sigma \to \nu f\Sigma$ and $e^{-f\sigma} \to \sqrt{Q}e^{-f\sigma}$ to exhibit Q as a new counting parameter in the path integral expression for $\langle U\rangle_Q$. Accordingly, the scaling dimension of the lowest-lying operator assumes the following form:

$$rE_Q = \Delta_Q = \sum_{j=-1}\frac{1}{Q^j}\Delta_j(Q(\Lambda_0 f)^4). \tag{35}$$

The leading order Δ_{-1} corresponds to $\tilde{\Delta}_Q$ and is given by the classical ground state energy on $\mathbb{R}\times S_r^3$, whereas the

[1] See [48] for a discussion of the power counting associated with the dilaton potential Eq. (27).

next-to-leading order Δ_0 is determined by the fluctuations around the classical trajectory. We refer the reader interested in the details of the approach to [69,70,74]. In the next section, we will determine the classical ground state energy $\tilde{\Delta}_Q/r$. Since in the near conformal regime the state-operator correspondence is only approximate, $\tilde{\Delta}_Q$ will be equal to $\tilde{\Delta}^*_Q$ plus corrections that disappear as the pion and dilaton masses vanish. As we shall see, deviations from conformality will be encoded in a set of contributions that depend on the spacetime geometry due to the lack of Weyl invariance.

V. LARGE CHARGE EXPANSION: LEADING ORDER

As anticipated in the previous section, the state-operator correspondence enables us to deduce the scaling dimension for the lowest-lying operator with (generalized) isospin charge Q. This is achieved by determining the energy associated with the vacuum structure inducing the superfluid phase transition. We therefore evaluate the Lagrangian (32) on the ansatz (10), obtaining

$$\begin{aligned}\mathcal{L}_\sigma[\Sigma_0,\sigma_0] = & -e^{-4f\sigma_0}\Lambda_0^4 - V(\sigma_0) - \frac{Re^{-2f\sigma_0}}{12f^2} \\ & + 2m_\pi^2\nu^2 X\cos\varphi e^{-f\sigma_0 y} \\ & + N_f\mu^2\nu^2 e^{-2f\sigma_0}\sin^2\varphi - a\nu^2 e^{-4f\sigma_0}\bar{\theta}^2, \end{aligned} \tag{36}$$

where σ_0 denotes the classical dilaton solution. It is worth noticing that, replacing $m_\pi \to \sqrt{2}m_\pi$ and $\mu \to \sqrt{2}\mu$, the resulting expression is identical to that found for two-color QCD at finite baryon density, as explored in [50]. Nevertheless, we further extend the results obtained in the previous work [50] by being able to solve for generic dilaton potentials (27) and mass deformations rather than concentrating on specific values of Δ and y.

The classical ground state energy is computed by solving the following EOMs:

$$\sin\varphi(N_f\mu^2 e^{-2f\sigma_0}\cos\varphi - m_\pi^2 X e^{-f\sigma_0 y}) = 0, \tag{37}$$

$$a e^{-4f\sigma_0}\bar{\theta} - m_\pi^2 \sin\alpha_i\cos\varphi e^{-f\sigma_0 y} = 0, \qquad i = 1,\ldots,N_f, \tag{38}$$

$$\begin{aligned}&\frac{Re^{-2f\sigma_0}}{6f} + 4af\nu^2 e^{-4f\sigma_0}\bar{\theta}^2 + 4f\Lambda_0^4 e^{-4f\sigma_0} - \left.\frac{\partial V(\sigma)}{\partial\sigma}\right|_{\sigma=\sigma_0} \\ &+ -2fN_f\mu^2\nu^2 e^{-2f\sigma_0}\sin^2\varphi - 2fym_\pi^2\nu^2 X\cos\varphi e^{-f\sigma_0 y} = 0,\end{aligned} \tag{39}$$

$$2N_f\mu\nu^2 e^{-2f\sigma_0}\sin^2\varphi = \frac{Q}{V}, \tag{40}$$

where the last equation defines the isospin charge density. To determine the classical ground state energy on the cylinder, we need to solve the above EOMs in the variables $\varphi, \alpha_i, \sigma_0$, and μ and plug the solution into Eq. (36). However, since the EOMs are transcendental equations it is not straightforward to find their exact solutions. We, therefore, overcome this issue by solving the EOMs perturbatively in positive powers of the parameters m_σ^2 and m_π^2. Specifically, we expand the variables as $x = x_0 + x_1 m_\sigma^2 + x_2 m_\pi^2 + x_3 m_\sigma^4 + x_4 m_\pi^4 + x_5 m_\sigma^2 m_\pi^2 + \mathcal{O}(m_\sigma^6, m_\pi^6, m_\sigma^4 m_\pi^2, m_\sigma^2 m_\pi^4)$ where $x = \{\mu, \varphi, \sigma_0, \alpha_i\}$ and determine the coefficients of the expansion by solving the EOMs order by order. The result reads

$$\begin{aligned}\tilde{\Delta}_Q = & \frac{\pi^2}{8f^2}(6N_f(f\nu\mu r)^2 + 1)\left(\frac{2N_f(f\nu\mu r)^2 - 1}{f^2\Lambda^4}\right) + m_\sigma^2\frac{\pi^2 2^{1-\Delta} r^{4-\Delta}}{(\Delta-4)\Delta f^2}\left(\frac{2N_f(f\nu\mu r)^2 - 1}{f^2\Lambda^4}\right)^{\Delta/2} \\ & - m_\pi^4 N_f\cos^2(\alpha(\theta))2^{2\gamma-3}\left(\frac{\pi\nu r^{\gamma+1}}{\mu r}\right)^2\left(\frac{2N_f(f\nu\mu r)^2 - 1}{f^2\Lambda^4}\right)^{2-\gamma} + \mathcal{O}(m_\sigma^4, m_\pi^8, m_\sigma^2 m_\pi^4),\end{aligned} \tag{41}$$

where μ is related to Q as

$$\mu r = \frac{(6\pi^4\nu^2 N_f)^{1/3} + \left(\sqrt{81f^6\Lambda^8 Q^2 - 6\pi^4\nu^2 N_f} + 9f^3\Lambda^4 Q\right)^{2/3}}{f(6\pi\nu^2 N_f)^{2/3}\left(\sqrt{81f^6\Lambda^8 Q^2 - 6\pi^4\nu^2 N_f} + 9f^3\Lambda^4 Q\right)^{1/3}}. \tag{42}$$

The first term in (41) represents the scaling dimension in the conformal limit $m_\pi = m_\sigma = 0$, which depends only on the dimensionless combination μr (42). The latter is determined by the value of the charge Q via Eq. (42) and, therefore, the first term in Eq. (41) is insensitive to the spacetime geometry. Noticeably, the leading correction in the pion mass is of order m_π^4, and its dependence on the geometry is tied to the anomalous dimension of the chiral condensate through the universal factor $r^{2(\gamma+1)}$. Remarkably, the whole θ-dependence is encoded in the factor $\cos^2(\alpha(\theta))$ with $\alpha(\theta)$ given in Eq. (18). The first term in the dilaton potential (27) redefines the cosmological constant as

$$\Lambda^4 \equiv \Lambda_0^4 + \frac{m_\sigma^2}{4f^2(4-\Delta)}. \tag{43}$$

The contribution stemming from the second term in the dilaton potential (27) has been expanded in powers of m_σ with the leading order quadratic in the dilaton mass. The latter exhibits a universal dependence on the radius of the sphere via the factor $r^{4-\Delta}$. It is interesting to further expand our results (41) in the large charge limit $Q(\Lambda_0 f)^4 \gg 1$, where we can make contact with the universal predictions of the large charge effective field theory (EFT) [64,67]. We have

$$\tilde{\Delta}_Q = \tilde{\Delta}_Q^* + \left(\frac{m_\sigma}{4\pi\nu}\right)^2 Q^{\frac{\Delta}{3}} B_1 + \left(\frac{m_\pi}{4\pi\nu}\right)^4 \cos^2(\alpha(\theta)) Q^{\frac{2}{3}(1-\gamma)} B_2 + \mathcal{O}(m_\sigma^4, m_\pi^8, m_\sigma^2 m_\pi^4), \tag{44}$$

where B_1 and B_2 read

$$B_1 = \frac{c_{2/3} 2^{9-2\Delta} 3^{\frac{\Delta}{2}-1} (\pi\nu r)^{4-\Delta} (c_{4/3} N_f)^{1-\frac{\Delta}{2}}}{(\Delta-4)\Delta} \left(1 - \frac{\Delta c_{2/3}}{4c_{4/3}} Q^{-2/3} + \mathcal{O}(Q^{-4/3})\right), \tag{45}$$

$$B_2 = -3^{4-\gamma} 2^{4\gamma-3} \pi^{2\gamma+2} c_{4/3}^{\gamma-4} N_f^{\gamma-1} (\nu r)^{2(\gamma+1)} \left(1 + \frac{(\gamma-4)c_{2/3}}{2c_{4/3}} Q^{-2/3} + \mathcal{O}(Q^{-4/3})\right), \tag{46}$$

while

$$\tilde{\Delta}_Q^* = c_{4/3} Q^{4/3} + c_{2/3} Q^{2/3} + \mathcal{O}(Q^0) \tag{47}$$

is the scaling dimension in the conformal limit at the leading order in the double scaling limit (33), which depends only on the dimensionless coefficients defined below

$$c_{4/3} = \frac{3}{8}\left(\frac{2\Lambda^2}{\pi N_f \nu^2}\right)^{2/3}, \quad c_{2/3} = \frac{1}{4f^2}\left(\frac{2\pi^2}{N_f \nu^2 \Lambda^4}\right)^{1/3}. \tag{48}$$

The conformal dimension $\tilde{\Delta}_Q^*$ exhibits the general structure predicted by the large charge EFT. The nonconformal corrections feature a characteristic Q-scaling, which has been made manifest in Eq. (44) and depends on the parameters γ and Δ encoding the explicit breaking of scale invariance.

VI. SYMMETRY BREAKING PATTERN AND SPECTRUM OF FLUCTUATIONS

We now move to determine first the symmetry breaking pattern and then the spectrum of the theory. Fixing the generalized isospin charge results in

$$\begin{aligned} &SU(N_f)_L \times SU(N_f)_R \times U(1)_V \overset{N_f^2-1}{\rightsquigarrow} SU(N_f)_V \times U(1)_V \\ &\longrightarrow SU\left(\frac{N_f}{2}\right)_u \times SU\left(\frac{N_f}{2}\right)_d \times U(1)_I \times U(1)_V \\ &\overset{\frac{N_f^2}{4}}{\rightsquigarrow} SU\left(\frac{N_f}{2}\right)_{ud} \times U(1)_V, \end{aligned} \tag{49}$$

where $\rightsquigarrow$ and $\longrightarrow$ denote, respectively, spontaneous and explicit breaking. The first stage is the usual chiral symmetry breaking with the Adler-Bell-Jackiw anomaly already taken into account in the breaking of the axial symmetry. The further explicit breaking is owed to the introduction of the isospin charge while the last spontaneous breaking is associated with pion condensation and the superfluid phase transition. In the absence of the dilaton, the spectrum of light modes is composed of $N_f^2/4$ massless Goldstone bosons with speed $v_G = 1$ that parameterize the coset $G/H = \frac{SU(N_f/2)_u \times SU(N_f/2)_d \times U(1)_I \times U(1)_V}{SU(N_f/2)_{ud} \times U(1)_V}$. These modes arrange themselves in the adjoint representation of the stability group $SU(N_f/2)_{udV} \times U(1)_V$ plus a singlet, which we denote as π_3 since it is associated with the spontaneous breaking of $U(1)_I$ i.e. to the third Pauli matrix in the $N_f = 2$ case. In addition, a pseudo-Goldstone mode stems from the would-be spontaneous breaking of $U(1)_A$, which we call the S (singlet) mode and it is related to the η'-meson [96]. As mentioned above, the $U(1)_A$ symmetry is quantum mechanically anomalous, and therefore, the latter mode acquires a mass proportional to the scale of the anomaly $\sqrt{a}$.

In what follows, we shall focus on the spectrum of Goldstone bosons since they control the large charge dynamics. Specifically, we are interested in analyzing how the spectrum of light modes changes when (near) conformal dynamics is realized through the dilaton dressing. Precisely, conformal invariance dictates the existence of a massless mode with speed $v_G = \frac{1}{\sqrt{d-1}} = \frac{1}{\sqrt{3}}$ [64,97]. As we shall see, the latter arises from the mixing between the singlet π_3 with the dilaton that acts as its "radial mode" and changes its speed from $v_G = 1$ to $v_G = \frac{1}{\sqrt{3}}$. We consider the hierarchy of scales $m_\pi, m_\sigma \ll \mu \ll 4\pi\nu$, which ensures the validity of chiral perturbation theory and assumes small deviation from conformality. To determine the fluctuations' spectrum, we expand around the vacuum solution as

$$\Sigma = e^{\frac{2i}{\sqrt{N_f}} S \mathbb{1}_{N_f}} e^{i\Omega} \Sigma_0 e^{-i\Omega^\dagger}, \tag{50}$$

where Σ_0 is the classical solution (8) while the fluctuations are organized in the matrix Ω as

$$\Omega = \begin{pmatrix} \pi & 0 \\ 0 & -\pi^T \end{pmatrix}. \tag{51}$$

Here, $\pi = \sum_{a=0}^{\dim \mathrm{G/H}} \pi^a t_a$ where the sum runs over all the generators of the coset G/H that we normalized as $\mathrm{Tr}\{t_a t_b\} = \frac{\delta_{ab}}{2}$. After some manipulations, we obtain

$$Tr\{\partial_\mu \Sigma \partial^\mu \Sigma^\dagger\} = 4\sin^2\varphi \partial_\mu \pi^a \partial^\mu \pi^a + 4\partial_\mu S \partial^\mu S, \tag{52}$$

$$\begin{aligned} Tr\{I\partial_0 \Sigma \Sigma^\dagger - I\Sigma^\dagger \partial_0 \Sigma\} &= 4i Tr\{I\partial_0 \nu\} \sin^2\varphi \\ &= 2i\sqrt{N_f}\partial_0 \pi^3 \sin^2\varphi, \end{aligned} \tag{53}$$

$$\begin{aligned} &Tr\{M\Sigma + M^\dagger \Sigma^\dagger\} \\ &\quad = 2\cos\varphi \left[X \cos\left(\frac{2}{\sqrt{N_f}} S\right) + Z \sin\left(\frac{2}{\sqrt{N_f}} S\right)\right], \end{aligned} \tag{54}$$

$$Tr\{\log\Sigma - \log\Sigma^\dagger\} = 4i\sqrt{N_f} S - 2i\sum_i^{N_f} \alpha_i, \tag{55}$$

where we defined $Z \equiv \sum_{i=1}^{N_f} \sin\alpha_i$. Finally, we expand the dilaton field around its background solution as $\sigma \to \sigma_0 + \hat\sigma(t, \mathbf{x})$. It is easy to show that the π_a modes corresponding to the Goldstone modes transforming according to the adjoint representation of $SU(N_f/2)$ have trivial dispersion relations $\omega = k$. On the other hand, the Goldstone boson, which is a singlet of $SU(N_f/2)$, mixes with the dilaton and the S. The corresponding dispersion relations are obtained by solving $\det D^{-1} = 0$, where the inverse propagator D^{-1} is given by

$$D^{-1} = \begin{pmatrix} \omega^2 - k^2 & i\omega\mu f\sqrt{N_f} & 0 \\ -i\omega\mu f\sqrt{N_f} & \frac{\omega^2-k^2}{8\nu^2 \sin^2\varphi} - M_\sigma^2 & \frac{1}{2} I_{\hat\sigma s} \\ 0 & \frac{1}{2} I_{\hat\sigma s} & \frac{\omega^2-k^2}{\sin^2\varphi} - M_s^2 \end{pmatrix}, \tag{56}$$

with

$$I_{\hat\sigma S} = \frac{f\mu^2\sqrt{N_f}(4a\mu^2\bar\theta N_f^2 e^{-2f\sigma_0\gamma} - m_\pi^4 XZ(3-\gamma))}{(\mu^4 N_f^2 e^{2f\sigma_0(1-\gamma)} - m_\pi^4 X^2)}, \tag{57}$$

$$\begin{aligned} M_\sigma^2 = \frac{\mu^2 N_f}{8\nu^2}\Bigg[&\frac{\Delta\mu^2 N_f m_\sigma^2 e^{-f(\Delta-2)\sigma}}{(\Delta-4)(\mu^4 N_f^2 - m_\pi^4 X^2 e^{2(\gamma-1)f\sigma})} \\ &+ \frac{2f^2(2\mu^2 N_f(\mu^2\nu^2 N_f e^{2f\sigma} - 4(a\nu^2\bar\theta^2 + \Lambda^4)) + ((\gamma-6)\gamma+7)\nu^2 m_\pi^4 X^2 e^{2\gamma f\sigma})}{m_\pi^4 X^2 e^{2\gamma f\sigma} - \mu^4 N_f^2 e^{2f\sigma}}\Bigg], \end{aligned} \tag{58}$$

$$M_S^2 = \frac{a\mu^4 N_f^3 + \mu^2 m_\pi^4 X^2 e^{2\gamma f\sigma_0}}{\mu^4 N_f^2 e^{2f\sigma_0} - m_\pi^4 X^2 e^{2\gamma f\sigma_0}}. \tag{59}$$

We pause to note that Eq. (58) is consistent with the Witten-Veneziano relation [98,99]. In fact, in the $m_\pi \to 0$ limit, M_S^2 reduces to

$$\lim_{\sigma_0\to 0, m_\pi \to 0} (59) \Rightarrow M_S^2 = aN_f. \tag{60}$$

The remaining dispersion relations are obtained by solving the equation $\det(D^{-1}) = 0$. The results describe two gapped modes $\omega_{1,2}$ with mass,

$$M_{1,2}^2 = -\frac{1}{2}\sin^2\varphi\left[M_S^2 + 8\nu^2 f^2\mu^2 N_f + 8\nu^2 M_\sigma^2 \pm \sqrt{(M_S^2 - 8\nu^2(f^2\mu^2 N_f + M_\sigma^2))^2 + 8\nu^2 I_{\hat\sigma S}^2}\right], \tag{61}$$

and a massless mode ω_3 with speed given by

$$v_3^2 = \frac{I_{\hat{\sigma}s}^2 - 4M_\sigma^2 M_S^2}{I_{\hat{\sigma}s}^2 - 4M_S^2(M_\sigma^2 + f^2 N_f \mu^2)}. \tag{62}$$

In parallel with the previous section, we determine the dispersion relations considering corrections in both m_σ^2 and m_π^2. According to this expansion, we obtain

$$\omega_i^2 = \omega_i^{2*} + \left(\frac{N_f \mu^2 \nu^2}{2\Lambda^4}\right)^{\frac{\Delta-2}{2}} m_\sigma^2 D_1(\omega_i^{2*}, \Delta) + \left(\frac{N_f \mu^2 \nu^2}{2\Lambda^4}\right)^{-\gamma-3} m_\pi^4 \cos^2(\alpha(\theta)) D_2(\omega_i^{2*}, \gamma) \\ + \mathcal{O}(m_\sigma^4, m_\pi^8, m_\sigma^2 m_\pi^4), \quad \text{for } i = 1, 2, 3. \tag{63}$$

The coefficients D_1 and D_2 read

$$D_1(\omega_i^{2*}, \Delta) = \frac{1}{12(\Delta-4) f^2 (\mu^2 \nu^2 N_f (a N_f (6 f^2 \mu^2 \nu^2 N_f + k^2 - \omega_i^{2*}) + 8 f^2 \Lambda^4 (2k^2 - 3\omega_i^{2*})) + 3\Lambda^4 (k^2 - \omega_i^{2*})^2)} \\ \times [a N_f (2 f^2 \mu^2 \nu^2 N_f ((3\Delta - 10) k^2 - 3(\Delta - 2)\omega_i^{2*}) - (k^2 - \omega_i^{2*})^2) \\ + 4 f^2 \Lambda^4 (k^2 - \omega_i^{2*})((3\Delta - 8) k^2 - 3\Delta \omega_i^{2*})], \tag{64}$$

$$D_2(\omega_i^{2*}, \gamma) = \frac{\mu^4 \nu^8 \Lambda^{-4(\gamma+4)} (\mu\nu)^{2\gamma} N_f^{\gamma+4}}{96(\mu^2 \nu^2 N_f (a N_f (k^2 - \omega_i^{2*}) + 8 f^2 \Lambda^4 (2k^2 - 3\omega_i^{2*})) + 6 a f^2 \mu^4 \nu^4 N_f^3 + 3\Lambda^4 (k^2 - \omega_i^{2*})^2)} \\ \times \bigg[-2(\gamma(3\gamma - 10) - 5) f^2 \Lambda^{4\gamma} \mu^{2-2\gamma} (k^2 - \omega_i^{2*}) (\nu^2 N_f)^{1-\gamma} (a \mu^2 \nu^2 N_f^2 + 2\Lambda^4 (k^2 - \omega_i^{2*})) \\ + 3(k^2 - \omega_i^{2*})^2 \left(\frac{\mu^2 \nu^2 N_f}{\Lambda^4}\right)^{-\gamma} (a \mu^2 \nu^2 N_f^2 + 2\Lambda^4 (k^2 - \omega_i^{2*})) - 16(\gamma - 1) f^2 \omega_i^{2*} \Lambda^{4\gamma} \mu^{2-2\gamma} (\nu^2 N_f)^{1-\gamma} \\ \times (a \mu^2 \nu^2 N_f^2 + 2\Lambda^4 (k^2 - \omega_i^{2*})) + \Lambda^{4\gamma} (\mu\nu)^{-2\gamma} N_f^{-\gamma} (4 f^2 \mu^2 \nu^2 N_f (k^2 - 3\omega_i^{2*}) + (k^2 - \omega_i^{2*})^2) \\ \times (6\Lambda^4 (k^2 + \mu^2 - \omega_i^{2*}) - a(\gamma - 7) \mu^2 \nu^2 N_f^2) \bigg], \tag{65}$$

while the dispersion relations in the conformal limit $m_\pi = m_\sigma = 0$ have the following simple form:

$$\omega_1^{2*} = k^2 + 6 f^2 \mu^2 \nu^2 N_f + 2 f \mu \nu \sqrt{N_f (9 f^2 \mu^2 \nu^2 N_f + 2k^2)}, \tag{66}$$

$$\omega_2^{2*} = k^2 + \frac{a \mu^2 \nu^2 N_f^2}{2\Lambda^4}, \tag{67}$$

$$\omega_3^{2*} = k^2 + 6 f^2 \mu^2 \nu^2 N_f - 2 f \mu \nu \sqrt{N_f (9 f^2 \mu^2 \nu^2 N_f + 2k^2)}, \tag{68}$$

where we can recognize the expected mode with a square mass of order a stemming from the axial anomaly as well as a gapped mode with mass $12 N_f f^2 \mu^2 \nu^2$ and a Goldstone boson with speed $v_3^2 = \frac{1}{3}$, as dictated by scale invariance. We conclude the section by providing explicit expression for $M_{1,2}^2$ and v_3^2,

$$v_3^2 = \frac{1}{3} + m_\sigma^2 \left(\frac{N_f \mu^2 \nu^2}{2\Lambda^4}\right)^{\Delta/2} \frac{\Lambda^4}{9 f^2 N_f^2 \mu^4 \nu^4} - m_\pi^4 \cos^2(\alpha(\theta)) \left(\frac{N_f \mu^2 \nu^2}{2\Lambda^4}\right)^{-\gamma-3} \frac{\mu^4 \nu^8 N_f^2}{144 \Lambda^{16}} (\gamma - 3)(\gamma + 1) + \mathcal{O}(m_\sigma^4, m_\pi^8, m_\sigma^2 m_\pi^4), \tag{69}$$

$$M_1^2 = 12N_f f^2\mu^2\nu^2 + m_\sigma^2\left(\frac{N_f\mu^2\nu^2}{2\Lambda^4}\right)^{\Delta/2}\frac{\Delta}{\Delta-4}\left(\frac{2\Lambda^4}{N_f\mu^2\nu^2}\right) - m_\pi^4\cos^2(\alpha(\theta))\left(\frac{N_f\mu^2\nu^2}{2\Lambda^4}\right)^{-\gamma-3}\frac{f^2\mu^6\nu^{10}N_f^3}{8\Lambda^{16}}(\gamma^2-6\gamma+7) + \mathcal{O}(m_\sigma^4, m_\pi^8, m_\sigma^2 m_\pi^4), \tag{70}$$

$$M_2^2 = \frac{a\mu^2\nu^2N_f^2}{2\Lambda^4} - m_\sigma^2\left(\frac{N_f\mu^2\nu^2}{2\Lambda^4}\right)^{\Delta/2}\frac{a}{6(\Delta-4)f^2\mu^2\nu^2} - m_\pi^4\cos^2(\alpha(\theta))\left(\frac{N_f\mu^2\nu^2}{2\Lambda^4}\right)^{-\gamma-3}\frac{\mu^6\nu^8N_f^2}{96\Lambda^{20}}(a(\gamma-4)\nu^2N_f^2-6\Lambda^4) + \mathcal{O}(m_\sigma^4, m_\pi^8, m_\sigma^2 m_\pi^4). \tag{71}$$

VII. CASIMIR ENERGY CONTRIBUTION TO Δ_Q IN THE CONFORMAL LIMIT

As discussed in Sec. IV, in the conformal limit $m_\pi = m_\sigma = 0$, our results (44) correspond to the leading contribution to the conformal dimension Δ_Q^* of the lowest-lying charge Q operator in the double scaling limit (33). However, as has been first shown in [64], Δ_Q can also be computed in the strongly coupled regime by constructing an EFT for the relativistic Goldstone modes stemming from the spontaneous symmetry breaking induced by fixing the charge. In $d = 4$ dimensions, the large charge EFT predicts [64,75]

$$\Delta_Q^* = k_{4/3}Q^{4/3} + k_{2/3}Q^{2/3} + k_0\log Q + \mathcal{O}(Q^0), \tag{72}$$

where the coefficients $k_{4/3}$ and $k_{2/3}$ are related to the Wilson coefficients of the EFT and cannot, therefore, be computed within the EFT approach. The calculated coefficients $c_{4/3}$ and $c_{2/3}$ given in Eq. (48) can be seen as the leading contribution to $k_{4/3}$ and $k_{2/3}$ in a perturbative expansion of the latter around $(\Lambda_0 f)^4 = 0$ [74]. On the other hand, the coefficient k_0 is a purely quantum contribution related to the Casimir energy of the relativistic Goldstone bosons.[2] Importantly, its value is universal being entirely determined by symmetry and the number of spacetime dimensions. In particular, it can be computed exactly from the knowledge of the low-energy spectrum. In fact, consider the low-energy action for a Goldstone mode χ,

$$S_G = \int_{\mathcal{M}} \mathrm{d}t\,\mathrm{d}\mathbf{x}\left(\frac{1}{2}(\partial_t\chi)^2 + \frac{v_G^2}{2}(\boldsymbol{\nabla}\chi)^2\right). \tag{73}$$

The corresponding Casimir energy is given by

$$\begin{aligned} E_{\text{Casimir}} &= \frac{1}{2}\mathrm{Tr}\{\log(-\partial_t^2 - v_G^2\nabla^2)\} \\ &= \frac{1}{4\pi}\int_{-\infty}^{\infty}\mathrm{d}\omega\sum_{\mathbf{p}}\log(\omega^2 + v_G^2E^2(\mathbf{p})) \\ &= \frac{v_G}{2}\sum_{\mathbf{p}}E(\mathbf{p}). \end{aligned} \tag{74}$$

Here, $E^2(\mathbf{p})$ denotes the eigenvalues of the Laplacian operator on S^3. The above contribution scales as Q^0 and exhibits a pole for $d \to 4$ in dimensional regularization. The latter is related to a $\log Q$ term with a universal coefficient $-\frac{v_G}{48}$ stemming from the renormalization of the vacuum energy [75]. Hence, we simply need to sum the contributions of the various Goldstone bosons in order to calculate k_0. The symmetry breaking pattern in the chiral limit reads

$$\begin{aligned} &SU(N_f)_L \times SU(N_f)_R \times U(1)_V \times U(1)_A \\ &\to SU\left(\frac{N_f}{2}\right)_{uL} \times SU\left(\frac{N_f}{2}\right)_{dL} \times SU\left(\frac{N_f}{2}\right)_{uR} \\ &\quad \times SU\left(\frac{N_f}{2}\right)_{dR} \times U(1)_I \times U(1)_V \\ &\overset{\frac{3}{4}N_f^2-2}{\rightsquigarrow} SU\left(\frac{N_f}{2}\right)_{ud} \times U(1)_V. \end{aligned} \tag{75}$$

The resulting $\frac{3}{4}N_f^2 - 2$ Goldstone bosons have speed $v_G = 1$ except the π^3 mode which has $v_G = \frac{1}{\sqrt{3}}$. We therefore obtain

$$k_0 = -\frac{1}{48}\left(\frac{1}{\sqrt{3}} + \frac{3}{4}N_f^2 - 3\right). \tag{76}$$

VIII. CONCLUSIONS

We uncovered near conformal properties of finite isospin density QCD on a nontrivial gravitational background. Specifically, we determined the classical ground state

[2] The value of k_0 can also be obtained by computing the next-to-leading order Δ_0 of the expansion (35).

energy $\tilde{\Delta}_Q/r$ with r the radius of $\mathbb{R} \times S_r^3$ via the semiclassical large charge expansion. In the conformal limit, this energy maps, via state-operator correspondence, into the scaling dimension $\tilde{\Delta}_Q^*$ of the lowest-lying operator of fixed isospin charge Q.

One of our main results given in (3) is the determination of the leading near conformal corrections to $\tilde{\Delta}_Q^*$ at the lower boundary of the QCD conformal window. We showed that the characteristic Q-scalings due to the near conformal corrections are induced by the quark mass operator anomalous dimension γ as well as the conformal dimension Δ of the operator responsible for dynamically deforming QCD away from the conformal window. Our results and methodology work as a template to obtain similar results for QCD-like theories, such as two-color QCD at nonzero baryon density.

Additionally, we determined the pattern of symmetry breaking, the associated physical spectrum, and their dispersion relations. These latter results will also help to determine the next-to-leading order large charge contributions. Last but not least, we discussed the $\mu - \theta$ QCD phase diagram.

ACKNOWLEDGMENTS

The work of J. B. was supported by the World Premier International Research Center Initiative (WPI Initiative), MEXT, Japan; and also supported by the JSPS KAKENHI Grant No. JP23K19047. The work of F. S. is partially supported by the Carlsberg Foundation, Grant No. CF22-0922. A. D. A. expresses sincere appreciation to the University of Southern Denmark and D-IAS for their hospitality during the crucial final stages of the work.

[1] Tom Banks and A. Zaks, On the phase structure of vector-like gauge theories with massless fermions, Nucl. Phys. **B196**, 189 (1982).
[2] Giacomo Cacciapaglia, Claudio Pica, and Francesco Sannino, Fundamental composite dynamics: A review, Phys. Rep. **877**, 1 (2020).
[3] Francesco Sannino and Kimmo Tuominen, Orientifold theory dynamics and symmetry breaking, Phys. Rev. D **71**, 051901 (2005).
[4] Dennis D. Dietrich and Francesco Sannino, Conformal window of SU(N) gauge theories with fermions in higher dimensional representations, Phys. Rev. D **75**, 085018 (2007).
[5] Byung Su Kim, Deog Ki Hong, and Jong-Wan Lee, Into the conformal window: Multirepresentation gauge theories, Phys. Rev. D **101**, 056008 (2020).
[6] Thomas A. Ryttov and Robert Shrock, Higher-loop corrections to the infrared evolution of a gauge theory with fermions, Phys. Rev. D **83**, 056011 (2011).
[7] Heinz Pagels, Departures from chiral symmetry: A review, Phys. Rep. **16**, 219 (1975).
[8] Thomas A. Ryttov and Francesco Sannino, Supersymmetry inspired QCD beta function, Phys. Rev. D **78**, 065001 (2008).
[9] Thomas A. Ryttov, Consistent perturbative fixed point calculations in QCD and supersymmetric QCD, Phys. Rev. Lett. **117**, 071601 (2016).
[10] Anna Hasenfratz, Claudio Rebbi, and Oliver Witzel, Gradient flow step-scaling function for SU(3) with twelve flavors, Phys. Rev. D **100**, 114508 (2019).
[11] Thomas Appelquist, George T. Fleming, and Ethan T. Neil, Lattice study of conformal behavior in SU(3) Yang-Mills theories, Phys. Rev. D **79**, 076010 (2009).
[12] Thomas Appelquist, George T. Fleming, and Ethan T. Neil, Lattice study of the conformal window in QCD-like theories, Phys. Rev. Lett. **100**, 171607 (2008); Phys. Rev. Lett. **102**, 149902(E) (2009).
[13] T. Appelquist, G. T. Fleming, M. F. Lin, E. T. Neil, and D. A. Schaich, Lattice simulations and infrared conformality, Phys. Rev. D **84**, 054501 (2011).
[14] Ting-Wai Chiu, Improved study of the β-function of $SU(3)$ gauge theory with $N_f = 10$ massless domain-wall fermions, Phys. Rev. D **99**, 014507 (2019).
[15] Claudio Pica and Francesco Sannino, UV and IR zeros of gauge theories at the four loop order and beyond, Phys. Rev. D **83**, 035013 (2011).
[16] Anna Hasenfratz, Ethan T. Neil, Yigal Shamir, Benjamin Svetitsky, and Oliver Witzel, Infrared fixed point of the SU(3) gauge theory with $N_f = 10$ flavors, Phys. Rev. D **108**, L071503 (2023).
[17] V. L. Berezinsky, Destruction of long range order in one-dimensional and two-dimensional systems having a continuous symmetry group. I. Classical systems, Sov. Phys. JETP **32**, 493 (1971).
[18] J. M. Kosterlitz and D. J. Thouless, Ordering, metastability and phase transitions in twodimensional systems, J. Phys. C **6**, 1181 (1973).
[19] J. M. Kosterlitz, The critical properties of the two-dimensional xy model, J. Phys. C **7**, 1046 (1974).
[20] V. A. Miransky and Koichi Yamawaki, Conformal phase transition in gauge theories, Phys. Rev. D **55**, 5051 (1997); Phys. Rev. D **56**, 3768(E) (1997).
[21] V. A. Miransky, Dynamics of spontaneous chiral symmetry breaking and continuum limit in quantum electrodynamics, Nuovo Cimento A **90**, 149 (1985).
[22] Thomas Appelquist, John Terning, and L. C. R. Wijewardhana, The zero temperature chiral phase transition in SU(N) gauge theories, Phys. Rev. Lett. **77**, 1214 (1996).
[23] Holger Gies and Joerg Jaeckel, Chiral phase structure of QCD with many flavors, Eur. Phys. J. C **46**, 433 (2006).

[24] Francesco Sannino, Jumping dynamics, Mod. Phys. Lett. A **28**, 1350127 (2013).

[25] Bob Holdom, Raising condensates beyond the ladder, Phys. Lett. B **213**, 365 (1988).

[26] Bob Holdom, Continuum limit of quenched theories, Phys. Rev. Lett. **62**, 997 (1989).

[27] Andrew G. Cohen and Howard Georgi, Walking beyond the rainbow, Nucl. Phys. **B314**, 7 (1989).

[28] Giacomo Cacciapaglia and Francesco Sannino, Evidence for complex fixed points in pandemic data, arXiv: 2009.08861.

[29] Michele Della Morte, Domenico Orlando, and Francesco Sannino, Renormalization group approach to pandemics: The COVID-19 case, Front. Phys. **8**, 144 (2020).

[30] Giacomo Cacciapaglia, Corentin Cot, and Francesco Sannino, Second wave COVID-19 pandemics in Europe: A temporal playbook, Sci. Rep. **10**, 15514 (2020).

[31] Chung Ngoc Leung, S. T. Love, and William A. Bardeen, Spontaneous symmetry breaking in scale invariant quantum electrodynamics, Nucl. Phys. **B273**, 649 (1986).

[32] William A. Bardeen, Chung Ngoc Leung, and S. T. Love, The dilaton and chiral symmetry breaking, Phys. Rev. Lett. **56**, 1230 (1986).

[33] Koichi Yamawaki, Masako Bando, and Ken-iti Matumoto, Scale invariant technicolor model and a technidilaton, Phys. Rev. Lett. **56**, 1335 (1986).

[34] Francesco Sannino and Joseph Schechter, Chiral phase transition for SU(N) gauge theories via an effective Lagrangian approach, Phys. Rev. D **60**, 056004 (1999).

[35] Sidney Coleman, *Aspects of Symmetry: Selected Erice Lectures* (Cambridge University Press, Cambridge, England, 1985).

[36] Deog Ki Hong, Stephen D. H. Hsu, and Francesco Sannino, Composite Higgs from higher representations, Phys. Lett. B **597**, 89 (2004).

[37] Dennis D. Dietrich, Francesco Sannino, and Kimmo Tuominen, Light composite Higgs from higher representations versus electroweak precision measurements: Predictions for CERN LHC, Phys. Rev. D **72**, 055001 (2005).

[38] Thomas Appelquist and Yang Bai, A light dilaton in walking gauge theories, Phys. Rev. D **82**, 071701 (2010).

[39] Zackaria Chacko and Rashmish K. Mishra, Effective theory of a light dilaton, Phys. Rev. D **87**, 115006 (2013).

[40] Shinya Matsuzaki and Koichi Yamawaki, Dilaton chiral perturbation theory: Determining the mass and decay constant of the technidilaton on the lattice, Phys. Rev. Lett. **113**, 082002 (2014).

[41] Martin Hansen, Kasper Langæble, and Francesco Sannino, Extending chiral perturbation theory with an isosinglet scalar, Phys. Rev. D **95**, 036005 (2017).

[42] Maarten Golterman and Yigal Shamir, Low-energy effective action for pions and a dilatonic meson, Phys. Rev. D **94**, 054502 (2016).

[43] Oscar Catà and Christoph Müller, Chiral effective theories with a light scalar at one loop, Nucl. Phys. **B952**, 114938 (2020).

[44] Maarten Golterman, Ethan T. Neil, and Yigal Shamir, Application of dilaton chiral perturbation theory to $N_f = 8$, SU(3) spectral data, Phys. Rev. D **102**, 034515 (2020).

[45] Thomas Appelquist, James Ingoldby, and Maurizio Piai, Nearly conformal composite Higgs model, Phys. Rev. Lett. **126**, 191804 (2021).

[46] Thomas Appelquist, James Ingoldby, and Maurizio Piai, Dilaton effective field theory, Universe **9**, 10 (2023).

[47] O. Cat‘a, R. J. Crewther, and Lewis C. Tunstall, Crawling technicolor, Phys. Rev. D **100**, 095007 (2019).

[48] Thomas Appelquist, James Ingoldby, and Maurizio Piai, Dilaton potential and lattice data, Phys. Rev. D **101**, 075025 (2020).

[49] Domenico Orlando, Susanne Reffert, and Francesco Sannino, Charging the conformal window, Phys. Rev. D **103**, 105026 (2021).

[50] Jahmall Bersini, Alessandra D'Alise, Francesco Sannino, and Matías Torres, Charging the conformal window at nonzero θ angle, Phys. Rev. D **107**, 125024 (2023).

[51] Jahmall Bersini, Alessandra D'Alise, Matias Torres, and Francesco Sannino, The dilatonic dynamics of baryonic crystals, branes and spheres, arXiv:2310.04083.

[52] Oleg Antipin, Matin Mojaza, and Francesco Sannino, Light dilaton at fixed points and ultra light scale super Yang mills, Phys. Lett. B **712**, 119 (2012).

[53] Roman Marcarelli, Nicholas Miesch, and Ethan T. Neil, Mass-induced confinement near the sill of the conformal window, Phys. Rev. D **107**, 076011 (2023).

[54] James Ingoldby, Hidden conformal symmetry from eight flavors, Proc. Sci. LATTICE2023 (**2024**) 091 [arXiv: 2401.00267].

[55] Thomas Appelquist, James Ingoldby, and Maurizio Piai, Dilaton potential and lattice data, Phys. Rev. D **101**, 075025 (2020).

[56] T. Appelquist *et al.*, Nonperturbative investigations of SU(3) gauge theory with eight dynamical flavors, Phys. Rev. D **99**, 014509 (2019).

[57] Thomas Appelquist, James Ingoldby, and Maurizio Piai, Analysis of a dilaton EFT for lattice data, J. High Energy Phys. 03 (2018) 039.

[58] Yigal Shamir and Maarten Golterman, Dilaton chiral perturbation theory and application, Proc. Sci. LATTICE2021 (**2022**) 372.

[59] Maarten Golterman and Yigal Shamir, Explorations beyond dilaton chiral perturbation theory in the eight-flavor SU(3) gauge theory, Phys. Rev. D **102**, 114507 (2020).

[60] Andrew Freeman, Maarten Golterman, and Yigal Shamir, Dilaton chiral perturbation theory at next-to-leading order, Phys. Rev. D **108**, 074506 (2023).

[61] Maarten Golterman and Yigal Shamir, Fits of SU(3) $N_f = 8$ data to dilaton-pion effective field theory, Proc. Sci. LATTICE2019 (**2019**) 130 [arXiv:1910.10331].

[62] Maarten Golterman and Yigal Shamir, Large-mass regime of the dilaton-pion low-energy effective theory, Phys. Rev. D **98**, 056025 (2018).

[63] John L. Cardy, Conformal invariance and universality in finite-size scaling, J. Phys. A **17**, L385 (1984).

[64] Simeon Hellerman, Domenico Orlando, Susanne Reffert, and Masataka Watanabe, On the CFT operator spectrum at large global charge, J. High Energy Phys. 12 (2015) 071.

[65] Debasish Banerjee, Shailesh Chandrasekharan, and Domenico Orlando, Conformal dimensions via large charge expansion, Phys. Rev. Lett. **120**, 061603 (2018).

[66] Domenico Orlando, Susanne Reffert, and Francesco Sannino, Near-conformal dynamics at large charge, Phys. Rev. D **101**, 065018 (2020).
[67] Luis Álvarez Gaumé, Domenico Orlando, and Susanne Reffert, Selected topics in the large quantum number expansion, Phys. Rep. **933**, 1 (2021).
[68] Simeon Hellerman, Daniil Krichevskiy, Domenico Orlando, Vito Pellizzani, Susanne Reffert, and Ian Swanson, The unitary Fermi gas at large charge and large N, arXiv:2311.14793.
[69] Oleg Antipin, Jahmall Bersini, Francesco Sannino, Zhi-Wei Wang, and Chen Zhang, Charging the O(N) model, Phys. Rev. D **102**, 045011 (2020).
[70] Oleg Antipin, Jahmall Bersini, and Pantelis Panopoulos, Yukawa interactions at large charge, J. High Energy Phys. 10 (2022) 183.
[71] Oleg Antipin, Alexander Bednyakov, Jahmall Bersini, Pantelis Panopoulos, and Andrey Pikelner, Gauge invariance at large charge, Phys. Rev. Lett. **130**, 021602 (2023).
[72] Oleg Antipin, Jahmall Bersini, Pantelis Panopoulos, Francesco Sannino, and Zhi-Wei Wang, Infinite order results for charged sectors of the Standard Model, J. High Energy Phys. 02 (2024) 168.
[73] Alexander Monin, David Pirtskhalava, Riccardo Rattazzi, and Fiona K. Seibold, Semiclassics, goldstone bosons and CFT data, J. High Energy Phys. 06 (2017) 011.
[74] Gil Badel, Gabriel Cuomo, Alexander Monin, and Riccardo Rattazzi, The epsilon expansion meets semiclassics, J. High Energy Phys. 11 (2019) 110.
[75] Gabriel Cuomo, A note on the large charge expansion in 4d CFT, Phys. Lett. B **812**, 136014 (2021).
[76] G. Arias-Tamargo, D. Rodriguez-Gomez, and J. G. Russo, The large charge limit of scalar field theories and the Wilson-Fisher fixed point at $\epsilon = 0$, J. High Energy Phys. 10 (2019) 201.
[77] Debasish Banerjee, Shailesh Chandrasekharan, Domenico Orlando, and Susanne Reffert, Conformal dimensions in the large charge sectors at the O(4) Wilson-Fisher fixed point, Phys. Rev. Lett. **123**, 051603 (2019).
[78] Debasish Banerjee and Shailesh Chandrasekharan, Subleading conformal dimensions at the O(4) Wilson-Fisher fixed point, Phys. Rev. D **105**, L031507 (2022).
[79] Hersh Singh, Large-charge conformal dimensions at the O(N) Wilson-Fisher fixed point, arXiv:2203.00059.
[80] Gabriel Cuomo, J. M. Viana Parente Lopes, José Matos, Júlio Oliveira, and Joao Penedones, Numerical tests of the large charge expansion, J. High Energy Phys. 05 (2024) 161.
[81] Edward Witten, Large N chiral dynamics, Ann. Phys. (N.Y.) **128**, 363 (1980).
[82] P. Di Vecchia and G. Veneziano, Chiral dynamics in the large n limit, Nucl. Phys. **B171**, 253 (1980).
[83] Davide Gaiotto, Zohar Komargodski, and Nathan Seiberg, Time-reversal breaking in QCD4, walls, and dualities in $2+1$ dimensions, J. High Energy Phys. 01 (2018) 110.
[84] Andrei V. Smilga, QCD at theta similar to pi, Phys. Rev. D **59**, 114021 (1999).
[85] Michel H. G. Tytgat, QCD at theta similar to pi reexamined: Domain walls and spontaneous *CP* violation, Phys. Rev. D **61**, 114009 (2000).
[86] D. T. Son and Misha A. Stephanov, QCD at finite isospin density, Phys. Rev. Lett. **86**, 592 (2001).
[87] D. T. Son and Misha A. Stephanov, QCD at finite isospin density: From pion to quark—antiquark condensation, Phys. At. Nucl. **64**, 834 (2001).
[88] Jahmall Bersini, Alessandra D'Alise, Francesco Sannino, and Matías Torres, The θ-angle and axion physics of two-color QCD at fixed baryon charge, J. High Energy Phys. 11 (2022) 080.
[89] Roger F. Dashen, Some features of chiral symmetry breaking, Phys. Rev. D **3**, 1879 (1971).
[90] Max A. Metlitski and Ariel R. Zhitnitsky, Theta-parameter in 2 color QCD at finite baryon and isospin density, Nucl. Phys. **B731**, 309 (2005).
[91] Walter D. Goldberger, Benjamin Grinstein, and Witold Skiba, Distinguishing the Higgs boson from the dilaton at the Large Hadron Collider, Phys. Rev. Lett. **100**, 111802 (2008).
[92] R. Rattazzi and A. Zaffaroni, Comments on the holographic picture of the Randall-Sundrum model, J. High Energy Phys. 04 (2001) 021.
[93] Thomas Appelquist, James Ingoldby, and Maurizio Piai, Dilaton EFT framework for lattice data, J. High Energy Phys. 07 (2017) 035.
[94] Yan-Ling Li, Yong-Liang Ma, and Mannque Rho, Chiral-scale effective theory including a dilatonic meson, Phys. Rev. D **95**, 114011 (2017).
[95] Yong-Liang Ma and Mannque Rho, Topology change, emergent symmetries and compact star matter, AAPPS Bull. **31**, 16 (2021).
[96] Paolo Di Vecchia and Francesco Sannino, The physics of the θ-angle for composite extensions of the standard model, Eur. Phys. J. Plus **129**, 262 (2014).
[97] D. T. Son, Low-energy quantum effective action for relativistic superfluids, arXiv:hep-ph/0204199.
[98] Edward Witten, Current algebra theorems for the U(1) Goldstone boson, Nucl. Phys. **B156**, 269 (1979).
[99] G. Veneziano, U(1) without instantons, Nucl. Phys. **B159**, 213 (1979).